Proceedings of the Institution of Civil Engineers
Structures & Buildings 160
January 2004 Issue SB1
Pages 1–9

Paper 13259

Received ???
Accepted ???

Keywords:
building structure & design/
composite structures/slabs & plates

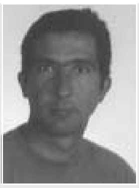

L. M. Bozzo
Polytechnic School, University of Girona

L. Torres
Polytechnic School, University of Girona

A proposed semi-prefabricated prestressed composite steel–concrete slab

L. M. Bozzo and L. Torres

This paper presents a semi-prefabricated prestressed composite slab, including experimental testing and appropriate numerical simulation tools, additioanlly design guidelines and a parametric study of the main variables. The system was applied for the first time in Spain during the construction of the library of the 'University of Lleida' covering 12 × 12 m spans with only 300 mm (*L*/40) total depth. This system considerably reduces the in situ work compared with other methods, allowing for large spans and two-way action. It is made up of three elements: (*a*) semi-prefabricated prestressed composite flat beams; (*b*) precast prestressed planks (namely preslabs); and (*c*) in situ reinforcement (transversal and negative) and topping concrete. Characterisation of element (*a*) using destructive experimental testing, as well as simple analytical and more precise numerical tools, using a layer model that includes constitutive equations for each material is included. A global analysis can be performed using a mixed finite element formulation including orthotropy. This last effect is important in this system, due to the different positions of the longitudinal and transversal reinforcement.

INTRODUCTION

Construction of composite steel–concrete structures in Spain started with the Tordera's bridge project by E. Torroja in the 1930. The structural logic of such composite solutions is clear, which is why they are widely-used and have undergone constant redevelopment. Analytical solutions for this type of beam have been available for many years. Nevertheless, in spite of their potential advantages there are very few composite steel–concrete slab structures, as well as very few precast two-way slabs.

When compared to linear systems the advantages of a two-way action include: greater flexibility in column distribution; and potential reduction of total depth and construction speed. Conventional slabs suffer from such disadvantages as the considerable high self-weight and a lower resistance to seismic action. This last disadvantage arises not only from the weight increase but also from the increased propensity to column fragile punching failure. As a consequence, it is widely accepted that in zones of high seismicity systems based on waffle slabs should not be recommended and often even permitted. It is for these reasons that over the passed 30 years in Peur composite steel–concrete reticulated slabs (*tridilosas*) have been actively developed allowing for the coverage of 20–30 m spans with live loads of 5 kN/m^2 at 500 mm of total depth and 1·5 kN/m^2 of self-weight (Fig. 1).[2] At present, this system is only economically suitable in countries, such as those of Latin America, where labour is relatively inexpensive.

Based on the work of Eng. M. Ollila in Finland, a prestressed semi-prefabricated composite steel–concrete slab has recently been constructed in Spain that potentially requires less in situ work in comparison to the *tridilosa*. A noteworthy example of a structure constructed with this novel system is the library of the University of Lleida, designed by the architects Gullichsen and Vormala. In this building, spans range from modules of 12 × 8 to 12 × 12 m, with total depths of only 300 mm. This paper describes the system, the experimental testing designed to characterise it, a numerical prediction of its long-term behaviour and examples of the influence of several parameters. The paper also contributes to ongoing development by proposing a finite element analysis method, based on the Reissner functional, which is able to simulate precisely orthotropic slab behaviour.

SYSTEM DESCRIPTION

The system is based on a framework of partially prefabricated (namely semi-prefabricated) prestressed composite steel–

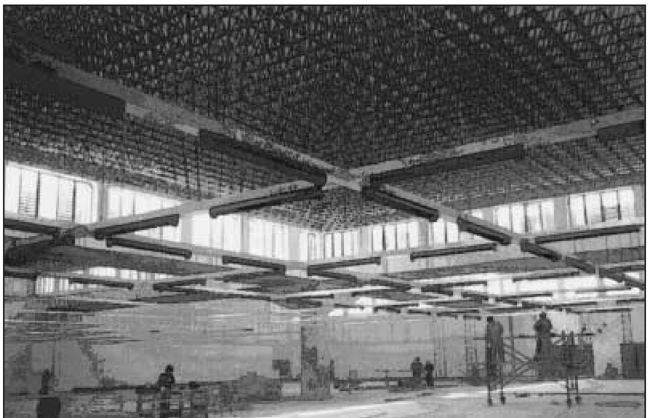

Fig. 1. Composite steel–concrete reticulated slab, Peru

Article number = 13259

concrete columns and the precast prestressed concrete planks (namely preslabs) supported on them. Preslabs act initially as permanent form for the cast-in-situ topping and subsequently together they act as a composite concrete slab (semi-precast slab). It is known that slab stress concentrates in the so-called 'column strips'. For this reason, the prestressed composite steel–concrete elements are located in these zones and the semi-precast slabs are supported on them. Fig. 2 presents a typical plan using the proposed system formed by the: (*a*) semi-prefabricated prestressed composite steel–concrete units; (*b*) precast prestressed concrete planks (preslabs); and (*c*) in situ topping concrete and reinforcement.

Since preslabs with lengths of more than 12 m are difficult to transport and mount, an 'optimal' plan of 12 × 12 m can be established for this slab system. The maximum practical span was established at 20 m . Using this system, the minimum structural depth was determined as (L/30–L/40). For example, structures at the University of Lleida have a span of 12 × 12 m and a total depth of 300 mm. The natural frequency of the system is in excess of 3 Hz, being satisfactory for the proposed use.

The composite steel–concrete beam is formed by a 'steel skeleton' consisting of a lightened beam obtained by cutting a HEB-320 mm (which allows passing transversal reinforcement improving the steel–concrete connection), welded to an 800 × 10 mm plate at its bottom end. Two lateral angular L 100 × 10 mm shapes are then welded to this bottom plate (see Fig. 3). The section is completed with N strands of 0·6' diameter, prestressed prior to casting the concrete. The number of prestressed cables varies, depending on the span and load. Beams using between 8 and 12 strands were constructed; the experimentally tested beam was made with 10 strands. This metallic skeleton and its corresponding prestressed concrete layer were constructed and prestressed at the ATEFOR company plant (Barcelona, Spain). The concrete of the precast zone is H50 (f_{ck} = 50 MPa) and the European designation of the structural steel is S275JR (f_y = 275 MPa).

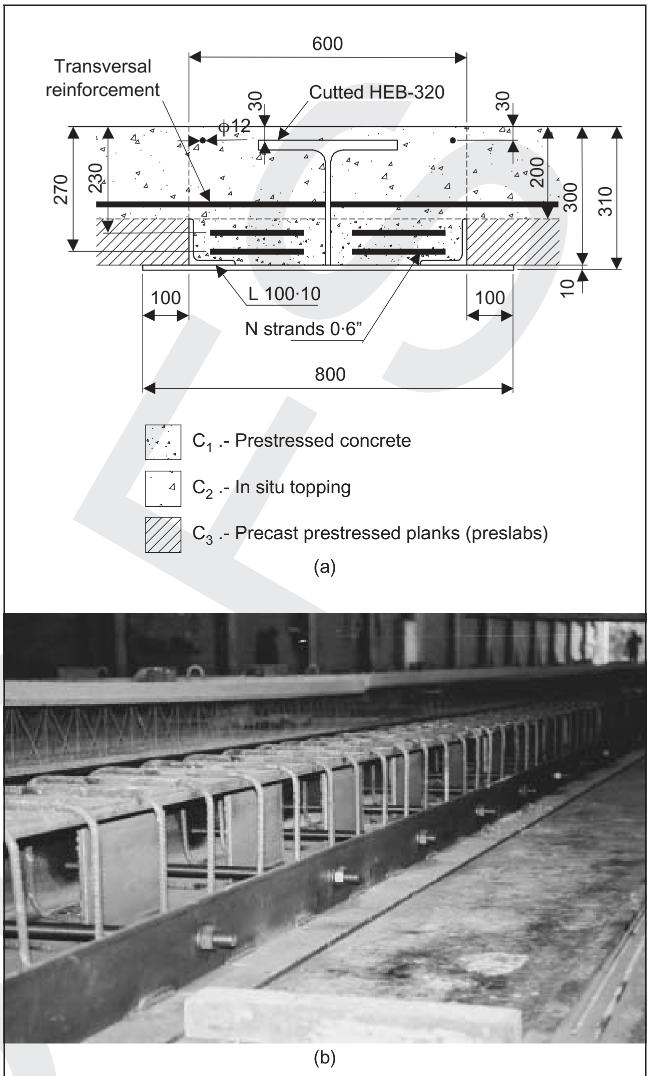

Fig. 3. (a) Beam section; (b) lateral view showing the lightened shape

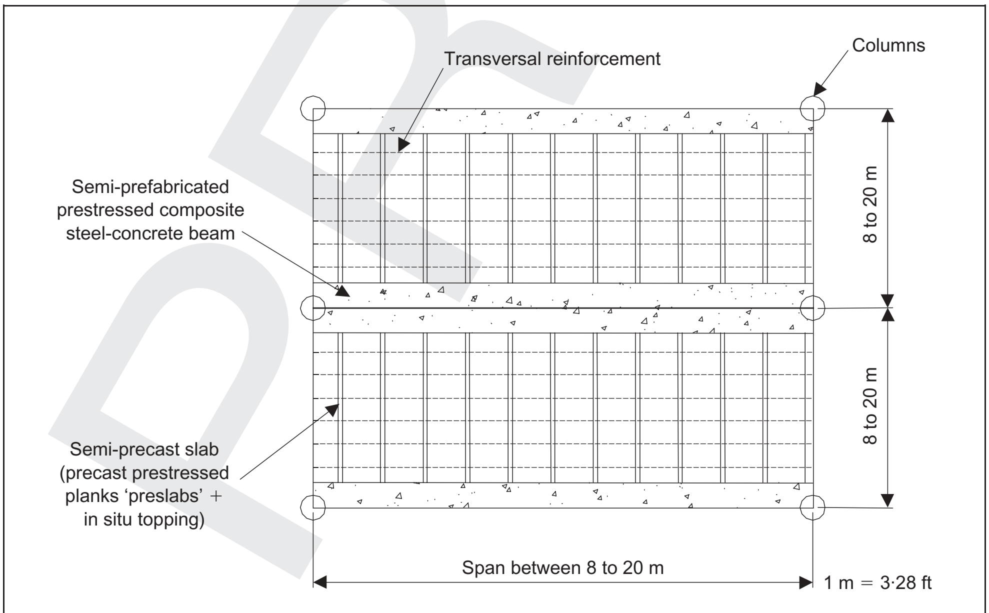

Fig. 2. Typical plan using the proposed system

Transversal 20 mm bars prestressed by a dynamometric key, to ensure good contact between steel and concrete, were used to improve the transference of the longitudinal prestressing to the metallic skeleton (see Fig. 4). Additional shear reinforcement was based on welded 12 mm diameter stirrups. These ∅ 12 mm connectors were welded at points of variable length, closer at the ends, providing ductile detail, such as is

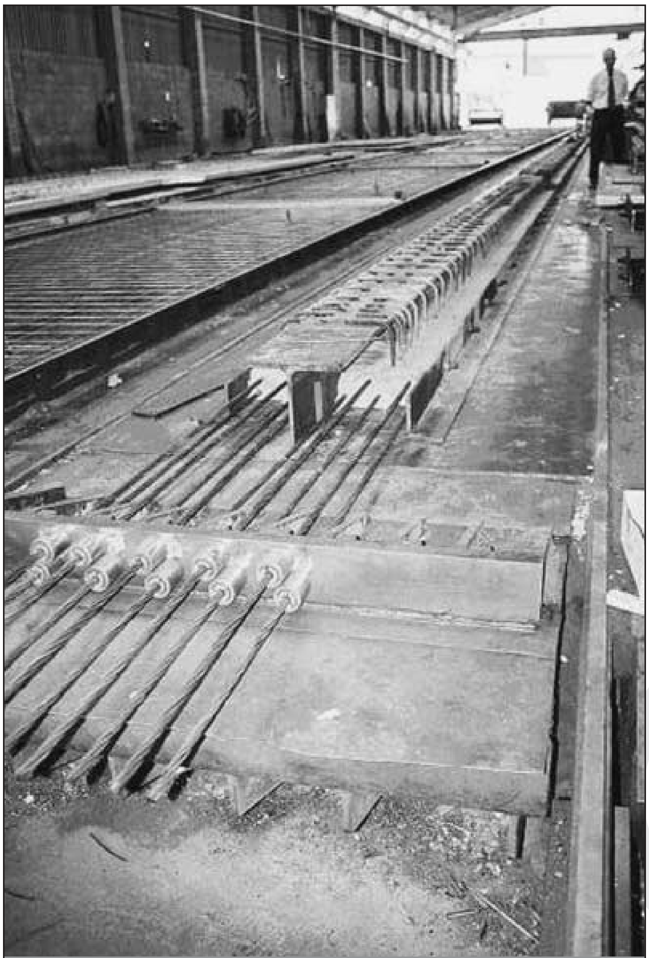

Fig. 4. Steel skeleton and manufacturing process after casting of bottom concrete layer

common in seismic regions. In general, the beam was prefabricated at the plant (Fig. 4) and transported to the construction site where the top part was completed. Basically, once the beam and transversal preslabs are mounted all that is required is the placement of transversal positive (if a two-way action is desired) and negative reinforcement. The steel beams can be assembled in such a way so as to obtain continuity and the columns can also be made as a composite to ensure better transference of shear force between slab and column, especially in zones of high seismicity (Fig. 5). Consequently, the execution time is reduced to that required to locate the cross-sectional transversal reinforcement points for positive moments in the precast slabs and for negative moments in the columns.

One difficulty obstructing an analysis of this system is the orthotropy caused by the cross-sectional cracking of preslabs, since they are prestressed in one direction only and the transversal in situ reinforcement is, necessarily, placed above the preslab. In relation to this, a precise finite element formulation that accounts for this effect in a relative simple model can be applied.[3,4]

The former Finnish system consisted of a similar metallic skeleton but with the following variations

(*a*) The bottom plate was corrugated to increase adherence to the lower concrete.

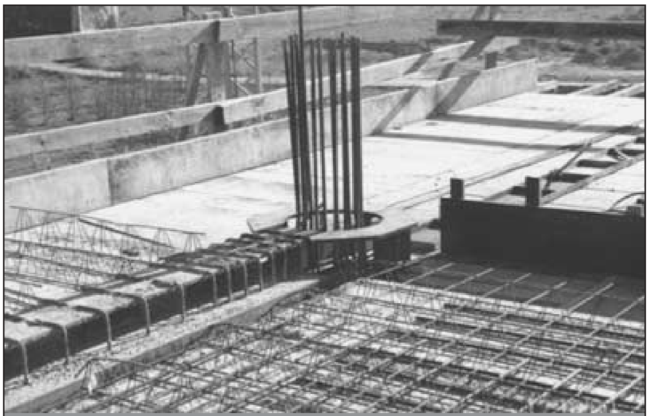

Fig. 5. Zone with ductile details and passing of reinforcement showing mechanical anchorage in the top flange of the half-HEB shape

(*b*) The section was formed from an angular steel shape or even a solid round bar and a discontinuous plate web.
(*c*) The stirrups were not welded to the steel skeleton.

The reasons for the differences between the adopted system and the one proposed by Olilla arose from the difficulty in finding corrugated plates with the required thickness in the local market, along with the advantages in inertia that were obtained using semi-wide-flange beams, in comparison to angular shapes. On the other hand, the buckling stability of the compressed flange during prestress transfer was greater in this proposed design and necessary because of the adopted level of prestressing (up to 2300 kN).

EXPERIMENTAL TEST AND SIMPLE ANALYTICAL PREDICTIONS

Due to the characteristics of the described system, it was considered appropriate to perform experimental testing to determine its ultimate strength and failure mode, as well as its behaviour under service conditions. The test of a complete slab was considered unnecessary since, quite apart from the significantly larger complexity that a full slab model would require, the main innovation of the system is concentrated in the linear elements.

Consequently, the criterion adopted was to test an element similar to the ones used in the construction of the library for the University of Lleida. Therefore a simply supported beam with a span of 8·30 m was tested. It fabrication consisted of a two-stage casting, simulating the 'real' construction sequence. In order to avoid zones of plain concrete (without reinforcement), two 12 mm diameter bars were added, completing a rectangular section of 600 × 300 mm. The top concrete layer had a compressive strength of 38 MPa on the day of the test, whereas the concrete in the prestressed zone reached a compressive strength of 47·3 MPa. The steel was of type S275JR, with a yield strength of 275 MPa. Previous analysis anticipated that bending failure would occur prior to shear or bonding failure between the steel skeleton and concrete.

The test was carried out in the General Test Laboratories run by the Catalan Government, Spain. The loading scheme corresponded to two concentrated loads applied at a distance of 3·0 m from each support, with a constant bending moment central zone. The mid-span deflection was registered during the tests and the environmental temperature was 21 ± 3°C.

The test was divided into three load phases: (*a*) application of the service load; (*b*) maintenance of the service load; and (*c*) application of the ultimate load.

The service load was determined to be 210 kN and was applied in 300 s under a constant speed of force increase. Afterwards, the unloading process was applied with a matching profile to determine the remaining deflection. Subsequently, the service load was applied again and maintained for 67 h 45 min to measure the initial time effect. The unloading process was redone following the same profile.

Deflections

Taking into account the applied load and the negligible presence of cracking due to the effect of prestressing, the instantaneous deflection can be determined in a simplified way, according to the following expression

$$\delta_{\max} = \frac{Fa}{24EI}(3L^2 - 4a^2) \tag{1}$$

where F (kN) is the value of each concentrated load (the total being $2F$); $a = 3$ m is distance of the load from the support; $L = 8{\cdot}3$ m is the total length of the beam; E (kN/mm^2) is the modulus of elasticity; and I (mm^4) is the moment of inertia of the transformed cross-section about its centroidal axis. Substituting these values gives δ_{max} mm

$$\delta\delta_{\max} = 2{\cdot}13 \times 10^{10}\frac{F}{EI} \tag{2}$$

Using this expression (suitable for the elastic behaviour) sufficient accuracy was obtained, as shown below. For this section, it appeared simpler to transform the concrete into an equivalent area of steel. Fig. 6 shows the transformed steel cross-section.

Figure 6 is obtained by means of the modular ratio $n = E_c/E_s$, corresponding to each type of concrete. The modulus of elasticity of the concrete is calculated following expressions

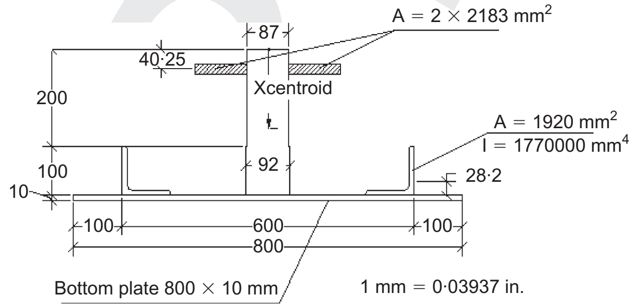

Fig. 6. Transformed steel cross-section

from CEB-FIP Model Code 1990,[5] leading to $n_1 = 6{\cdot}9$ and $n_2 = 6{\cdot}5$ for $f_{ck} = 38$ and 47·3 MPa, respectively. Consequently the moment of inertia of the transformed cross-section is $I = 46827 \times 10^4$ mm^4. Substituting into equation (2), we find that δ_{max} (mm) $= 0{\cdot}202F$

Taking into account the calculated service load of $2F = 210$ kN an instantaneous theoretical deflection of $\delta_{max} = 21{\cdot}21$ mm is obtained.

Figure 7(a) shows the load–deflection curve for the first stage of the loading and unloading test. A practically linear response is observed. The experimental deflection registered for a load of 210 kN was 23·27 mm with an error of 8·8% with respect to the theoretical one. In the unloading stage, a remaining deflection of only 0·68 mm was measured, verifying again the elastic linear response with hardly any slipping between metallic skeleton and concrete. Fig. 7(b) presents the variation of the deflection in the second phase of the test, where a load 210 kN was maintained for nearly 3 days, showing time-dependent effects.

Flexural ultimate load

Figure 8 shows the experimental results for the third phase of the test up to failure. A linear response was observed even for values higher than the supposed service load, up to 350 kN. This result is partly due to the fact that the design service load

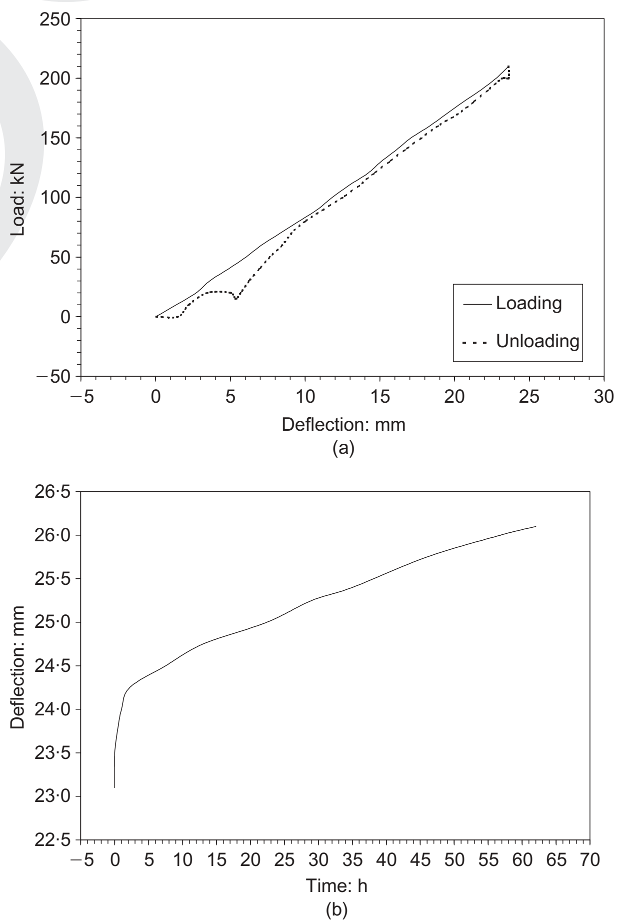

Fig. 7. Experimental results: (a) phase 1: short-term load; (b) phase 2: sustained service load for 67 h and 45 min

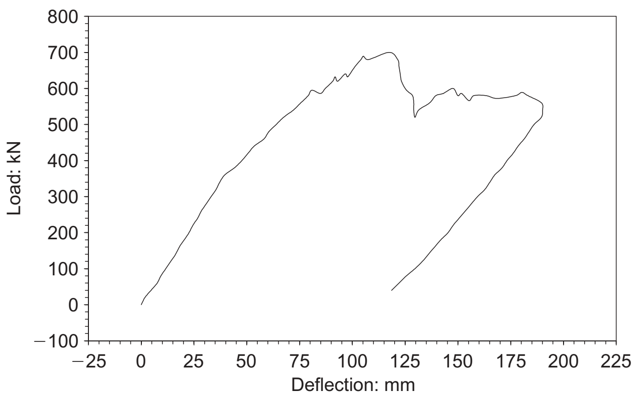

Fig. 8. Experimental results. Phase 3: ultimate load

was calculated taking into account the design prestressing losses. At approximately 600 kN pause for inspection was introduced, since the theoretical ultimate load was determined as being 630 kN. This load was calculated using the CEB methodology for concrete design[5] by means of the educational program DOMINIOS (which can be freely obtained through the University of Girona: http://emci.udg.es/mmcte/). Using this methodan ultimate bending moment of $M^* = 949{\cdot}0$ kN/m was obtained. In failure, the steel of the bottom plate has a strain $\varepsilon_s = 0{\cdot}0022$ and the top concrete fibre $\varepsilon_c = 0{\cdot}0035$.

This ultimate bending moment corresponds to a theoretical load value of $2F^* = 632{\cdot}6$ kN. The load obtained in the test was 704 kN, 10% higher than the theoretical one, and showed a fragile concrete compress failure (see Fig. 9; there is also a video in the aforementioned educational software). This fragile failure was caused by the small amount of compression reinforcement (2 ∅12 mm) added to the steel shape. Moreover, although the corrugated transversal bars welded to the HEB shape (Fig. 4) improved the steel–concrete bond, this was lower than in linear corrugated bars. When the beam was integrated in the proposed composite slabs, this situation would not necessarily occur, due to the much smaller concrete compression stresses experienced and to the confining action of the passive negative steel reinforcement, perpendicular to the axis of the beam.

Figure 10 presents a zone of the University of Lleida library, where the diaphanous spaces that can be obtained are illustrated. However, it should be emphasised that, through use of post-tensioned slabs, similar or even shallower depths can be obtained, the principle advantage of this solution is that it is semi-prefabricated, reducing both in situ work and execution time.

PRECISE NUMERICAL ANALYSIS AND EXAMPLES OF THE INFLUENCE OF SEVERAL FACTORS

Numerical modelling

This section reports a numerical analysis of the tested element under serviceability conditions. The model utilsed[6] is based on the generalised matrix formulation (GMF). The GMF is an extension of the classical matrix formulation for bars and allows for changes in bar stiffness (such as those produced by cracking or non-constant sections) and curved elements without further discretisation, similar to proposals made by other authors.[7–10] Time effects or other non-linearities (i.e. geometrical non-linearities or shores unable to resist tension forces) could be included. For calculation purposes, the cross-section is discretised into several layers; each may correspond to a different material. Deformations caused by shear force are neglected, and so the Navier–Bernouilli hypothesis applies.

Using this methodology, an 'exact' equilibrium between nodal and internal forces is established, so there is no need for either explicit shape functions or the discretisation of elements into shorter ones. The stiffness of the elements (bars) is determined with sectional behaviour taken into account; integrations along the members were carried out and, therefore, the integration rules applied provide the numerical precision.

Time analysis was performed by a general step-by-step procedure,[11] introducing tension increments at the middle of the calculation intervals. Cracking and multi-stage construction, among others, were considered, so that construction processes can be simulated, incorporating or suppressing sectional or structural parts consisting of various materials, with different ages and properties.

Comparison of numerical and experimental results

In the numerical representation, the initial time has been set as the instant at which the cables were prestressed and the bottom

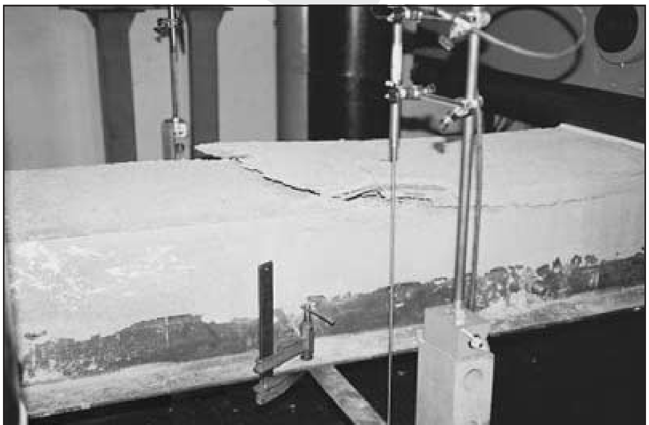

Fig. 9. Fragile failure due to concrete crashing

Fig. 10. Partial view of the University of Lleida library

concrete layer was cast. The transference was made 2 days later, and the beam was loaded to its self-weight but supported by shores preventing downward deflections. After 14 days the top concrete layer was applied, while maintaining identical conditions of support, and after 21 days, the shores are removed and the test load applied.

Evolution of concrete properties with time, creep, shrinkage and relaxation of the prestressed steel are determined using expressions recommended by the CEB-FIP MC-90,[5] assuming RH 55%.

The prestressing force was 1860 kN, corresponding to 70% of the characteristic steel tension strength. The total external applied load was $2F = 210$ kN. Although the real permanent load, which forms the main influence responsible for time dependent effects, was be lower, the simulation with constant load was designed to be simpler in order to understand the basic behaviour of the beam.

The curves presented show the mid-span deflection. The zero value corresponds to the instant immediately before the application of the concentrated loads (therefore the effect of self-weight and prestressing are included). The tension stiffening effect is negligible because of the presence of an important amount of tensioned steel combined with the prestressing action.

Figure 11 shows the comparison between experimental and numerical results for short-term service load. The response is practically linear, and a good adjustment between both curves is observed. The maximum experimental value was 23·3 mm while the numerically calculated value was 23·5 mm, showing an error of only 0·9%. The initial deflection due to prestressing and self-weight was 2·95 mm upwards.

The numerical results for stresses and strains for the mid-span cross-section indicate the presence of cracking in a small zone in the lower half of the bottom concrete layer, although this does not significantly modify the slope of the load–deflection diagram.

Figure 12 illustrates the response to a load sustained for 67 h and 45 min. Due to time effects, in this phase of the test, the deflection increases by 12% plotted against first stage deflection. Once again, the numerical model and the experimental values agree closely.

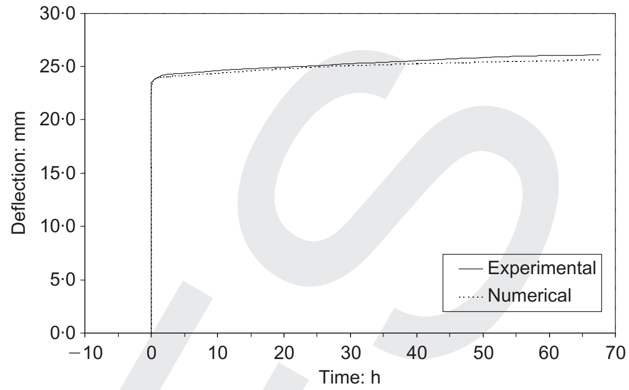

Fig. 12. Sustained service load (67 h and 45 min): comparison of experimental and numerical results

Long-term response: examples of the influence of several factors

This section presents a prediction of the long-term behaviour (5 years) of the element previously tested. Moreover, a parametric study shows the influence of several parameters, such as creep, shrinkage or the area of the steel profile, on the long-term behaviour of the beam. This parametric study provides design guidelines for the selection of the main parameters for considering the long-term response of the semi-prefabricated prestressed composite element in the proposed system.

Figure 13 shows the predicted evolution for long-term deflection, considering a sustained load over five years equivalent to the total service load. An increase of 50·6% is evident with respect to the instantaneous value obtained in the first stage of the test (23·5 mm). In the instantaneous test, the load was applied over 300 s and an important part of this delayed deflection (24%) already occurred within the first 3

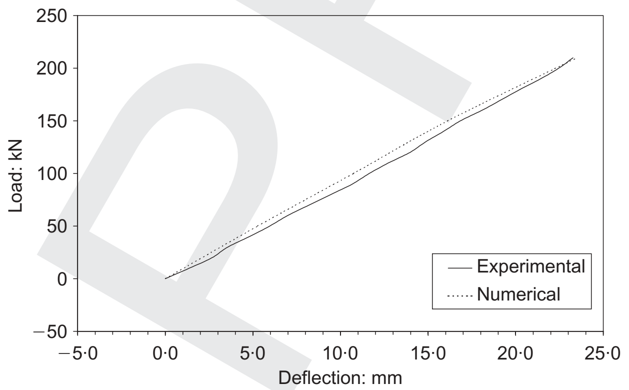

Fig. 11. Short-term service load: comparison of experimental and numerical results

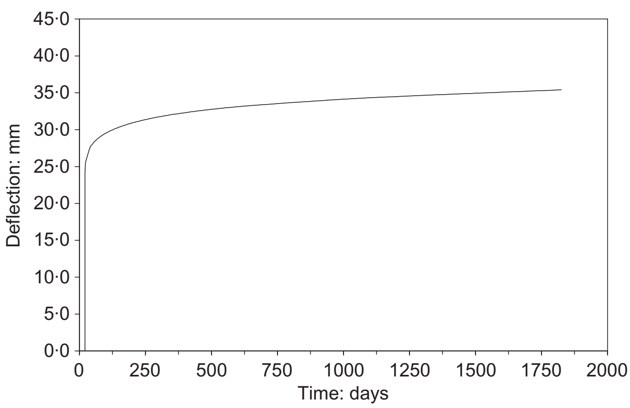

Fig. 13. Predicted long-term deflection for service load (5 years)

days, as was noted in the experimental results (Fig. 10). Also worth noting is the logical decreasing tendency of the slope over time, and a small increase in long-term deflection plotted against the instantaneous results.

Figure 14 illustrates the predicted stress evolution in the steel–concrete composite, taking into account a constant total service load applied at 21 days. The most relevant redistributions are observed in the upper fibres (concrete and steel), while in the lower fibres, the influence of initial prestressing results in a lower variation of stress. Moreover, the figure indicates the evolution in the stress of the prestressed strands over time.

Figure 15 presents numerical results of a long-term analysis, taking as a reference the values of Fig. 13, but suppressing alternately the effects of shrinkage and creep. A greater creep influence in the deflection value was observed, its effect being practically constant with time. On the other hand, the effect of suppressing shrinkage is smaller in the initial period but increases over time.

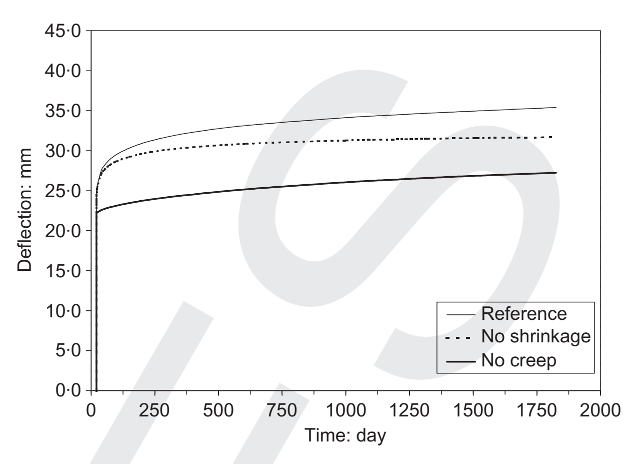

Fig. 15. Predicted long-term behaviour for service load: influence of creep and shrinkage of concrete

The initial deflection found in the numerical analysis, due to prestressing and self-weight application, was 3·15 mm when shrinkage is not taken into account and 1·95 mm when creep effects are omitted.

Figure 16 presents the results of reducing by half, first the value for the steel area of the bottom-welded plate and then the compressed flange of the steel shape. In both cases a significant increase was observed in the mid-span displacement from 35·40 mm in the reference case, up to 40·50 mm and 47·15 mm, respectively for each reduction.

As in the other cases, this deflection was due to the deformed configuration including self-weight and initial deflection due to prestressing. When the area of the bottom plate is reduced by 4000 mm^2 the calculated upwards vertical deflection prior to load application increases to 10·15 mm due to the greater effect of prestressing force and to the reduced stiffness of the section. When the area of the compressed flange of the steel shape is reduced by 3075 mm^2, the numerical analysis indicates a 7·4 mm downward deflection. However, in practice, this value will

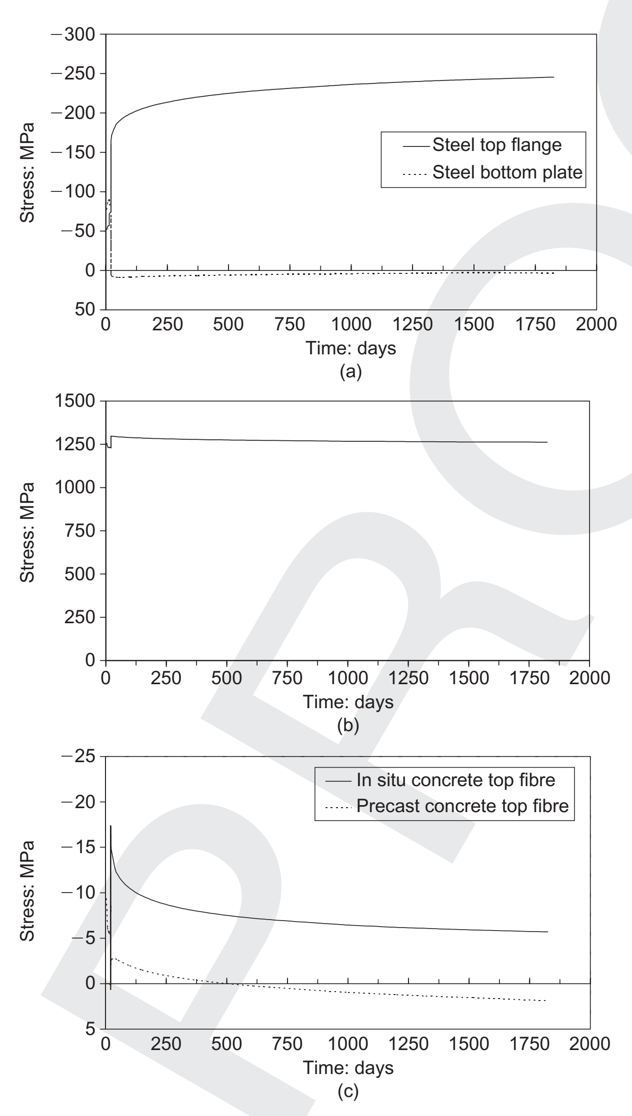

Fig. 14. Predicted redistribution of long-term stresses for service load (5 years): (a) steel shape; (b) prestressed steel lower layer; (c) concrete

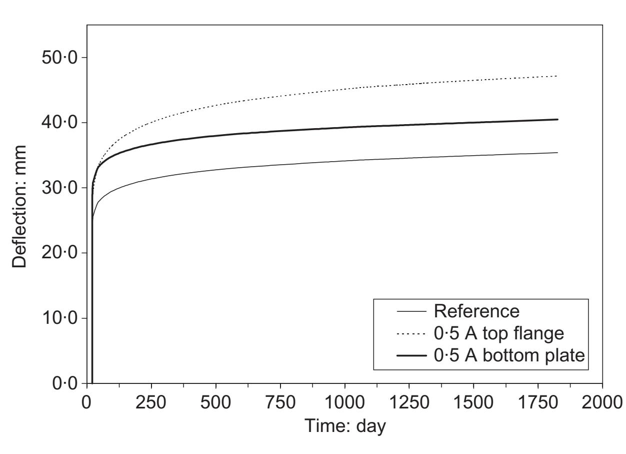

Fig. 16. Predicted long-term response for service load: influence of the structural steel area

not occur because the beam will either be in the prefabrication plant or supported by shores. Taking into account this real construction process, the initial calculated deflection at the moment before applying the external load is found to be 3·00 mm downwards. Compared with reducing the bottom plate, in this case the eccentricity of the prestressing force is less and the effect of the self-weight of the beam is more pronounced due to the section stiffness reduction.

Taking this effect into consideration, the final deflections recorded at the horizontal position vary from the indicated 40·50 to 30·35 mm when the bottom plate is reduced, and from 47·15 to 50·15 mm when the top plate is reduced. These results indicate that the horizontal lower steel plate may be reduced by 50% (i.e. a 5 mm plate can be used instead of a 10 mm one), without increasing the long-term maximum deflection.

Numerical finite element model

The global plate analysis was performed using a mixed finite element. The formulation is based on the Reissner functional, which provides a precise and robust means of analysing plates.[3,4] This functional for planar plates can be expressed as

$$\prod{}_r(w,\, M) = -U + \int_A \left(Q_x \frac{\partial w}{\partial x} + Q_y \frac{\partial w}{\partial y} - \bar{q} w \right) dA - \int_{S_o} \bar{Q}_n w dS + \int_{S_u} \left(M_{nn}\bar{\theta}_n + M_{ns}\bar{\theta}_s \right) dS \tag{4}$$

where U is the elastic internal energy $(\frac{1}{2}\mathrm{M}\ \mathrm{S}^{\mathrm{F}}\ \mathrm{M} + \mathrm{M}\bar{\chi} + \frac{1}{2}\mathrm{Q}\mathrm{S}^{\mathrm{c}}\mathrm{Q})$ including flexural and shear deformations as well as imposed curvatures $(\bar{\chi})$; Q_x and Q_y are the vertical shears normal to x and y axes, respectively; w is the vertical deflection; Q_n is the vertical shear normal to the n axes; M_{nn} and M_{ns} are the nn and ns moments. The node variables in this formulation are the vertical deflection, w, and the flexural, M_{xx}, M_{yy}, and torsional, M_{xy}, moments.

Minimising this functional with respect to the node variables provides a global equilibrium solution with the following advantages, compared to conventional potential energy formulations: (*a*) it reduces the order of the maximum derivative in the functional from two to one – allowing a robust element suitable for thick, as well as thin, plates to be formulated avoiding non-elegant procedures, such as reduced integration; (*b*) there is direct representation of flexural moments that are of more practical interest than rotations in conventional approaches; and (*c*) there is potential formulation of a high order element.

The proposed slab system has, as mentioned previously, two layers of positive reinforcement at different locations. The longitudinal layer is prestressed and the transversal one is placed in situ above the preslabs. This characteristic makes the use of an orthotropic formulation representation such as the following, necessary

$$\begin{Bmatrix} M_{xx} \\ M_{yy} \\ M_{xy} \\ Q_{xz} \\ Q_{yz} \end{Bmatrix} = \begin{bmatrix} \dfrac{E_x t^3}{12(1-n\mu_{yx}^2)} & \dfrac{\mu_{yx} E_x t^3}{12(1-n\mu_{yx}^2)} & 0 & 0 & 0 \\ \dfrac{\mu_{xy} E_x t^3}{12(1-n\mu_{yx}^2)} & \dfrac{E_x t^3}{12n(1-n\mu_{yx}^2)} & 0 & 0 & 0 \\ 0 & 0 & \dfrac{kt^3}{12} G_{xy} & 0 & 0 \\ 0 & 0 & 0 & ktG_{xz} & 0 \\ 0 & 0 & 0 & 0 & ktG_{yz} \end{bmatrix} \times \begin{Bmatrix} \chi_{xx} \\ \chi_{yy} \\ \chi_{xy} \\ \gamma_{xz} \\ \gamma_{yz} \end{Bmatrix} \tag{5}$$

where $n = E_x/E_y = \mu_{xy}/\mu_{yx}$, μ is the Poisson's ratio for each direction; G is the shear modulus; k is a constant (usually set to 1·2) to improve the representation of shear deformations for thick slabs; and t is the gross thickness. For each direction, an equivalent thickness must be used as a function of the amount and location of the steel reinforcement providing a precise tool which can be used to analyse the proposed system.

Following the proposal by Graham and Scanlon,[12] the material properties can be obtained from the following

$$E_x = \alpha_x E_c \qquad E_y = \alpha_y E_c \tag{6}$$

where

$$\alpha_x = \frac{I_{ex}}{I_{gx}} \qquad \alpha_y = \frac{I_{ey}}{I_{gy}} \tag{7}$$

and I_{ex}, I_{ey} are the effective moments of inertia for a given point; and I_{gx}, I_{gy} are the corresponding gross moment of inertia.

CONCLUSION

This paper presented a structural system, utilsed intially in Spain, that allows spans with 12 × 12 m modules and total depths of 300 mm or L/40 to be used for conventional building loads. For highway over pass structures, this depth may be increased up to 600 mm or L/20. The system is made up of: (*a*) semi-prefabricated prestressed composite steel–concrete units; (*b*) precast prestressed planks (preslabs); and (*c*) in situ topping concrete and reinforcement. The article includes results from a characterisation test carried out in the General Test Laboratories of the Catalan Government, Spain for element (*a*) of the system.

The tests indicated that the structural element can be modelled with simple tools under service conditions (i.e. using a transformed homogeneous section) and using the CEB methodology for concrete design (CEB-FIP MC 90[5]) at failure. The metallic skeleton and the concrete worked perfectly together, slipping was not observed, even at failure.

The paper included a parametric study using a more precise method, which consisted of a layer model implemented in an extension of the matrix formulation for bars, and that was suitable for non-linear time-dependent analysis. It was used to analyse the influence of the main variables that determine long-term response of the composite elements, such as the upper and lower structural steel areas, shrinkage and creep. The study indicated that long-term deflections after 5 years are small and limited to 50·6% for the tested element. The most relevant redistribution of stress were observed for the upper fibres (concrete and steel), with a smaller variation in the lower ones. The areas of the compressed flange and the bottom plate of the structural steel shape have a considerable influence on the long-term response. Reducing them to half the initial value, a 3075 mm^2 reduction for the compressed flange, and 4000 mm^2 reduction for the bottom plate, increased the total long-term response by 33 and 14%, respectively (considering the initial upward deflection due to prestressing).

The paper also included further precise numerical tools. Global analysis can be performed using a mixed finite element formulation including orthotropy, which is an important element in this system due to the different positions of the longitudinal and transversal reinforcement.

REFERENCES

1. Beer H. La acción conjunta de la viga metálica y la losa de hormigón. Ciencia y Técnica, Argentina, Mayo, 1951.
2. Bozzo M. and Bozzo L. M. Losas reticulares mixtas. Proyecto, análisis y dimensionamiento, Ed. Reverté, 2003.
3. Bozzo L. M. *Análisis de losas planas empleando un elemento finito isoparamétrico mixto de 3 a 8 nudos*. Civil Engineering Thesis, National University of Engineering, Lima, Peru, 1986.
4. Murcia J. and Bozzo L. Análisis diferido de placas de hormigón armado y pretensado empleando elementos finitos mixtos. *Hormigón y Acero*, 1994, **194**, 17–28.
5. Comité Euro-International du Béton. *CEB - FIP Model Code* 1990, Thomas Telford, London, 1993.
6. Torres L., Lopez-Almansa F., Cahis X. and Bozzo L. M. A numerical model for sequential construction, repairing and strengthening of 2-D concrete frames. *Engineering Structures*, 2003, **25**, No. 3, 323–336.
7. Ghali A. and Elbadry M. Serviceability design of continuous prestressed concrete structures. *PCI Journal*, 1989, **34**, No. 1, 54–91.
8. Carol I. and Murcia J. Nonlinear time-dependent analysis of planar frames using an 'exact' formulation: I -theory, II - computer implementation for RC structures and examples. *Computers and Structures*, 1989, **33**, No. 1, 79–87, 89–102.
9. Marí A. R. *A General Method for the Analysis of Curved Beams and Space Frames*. Dept. of Construction Engineering, Technical University of Catalonia, Barcelona, Spain, 1985.
10. Molins C. and Roca P. Capacity of masonry arches and spatial frames. *Journal of Structural Engineering, ASCE*, 1998, **124**, No. 6, 653–663.
11. Ghali A. and Favre R. *Concrete Structures: Stresses and Deformations*. E&FN Spon, London, 1994.
12. Graham C. and Scanlon A. Deflections of concrete slabs under construction loading. *ACI SP-86, Deflections of Concrete Structures*, Detroit, 1985.

Please email, fax or post your discussion contributions to the secretary: email: mary.henderson@ice.org.uk; fax: +44 (0)20 665 2294; or post to Mary Henderson, Journals Department, Institution of Civil Engineers, 1–7 Great George Street, London SW1P 3AA.